#3

LOCKING PHENOMENA IN MICROWAVE OSCILLATORS WITH MISMATCHED LOADS

JOSEPH C. PITTS
WILLIAM F. WICKS
EDWARD E. DAVID, JR.

TECHNICAL REPORT NO. 175

SEPTEMBER 11, 1950

RESEARCH LABORATORY OF ELECTRONICS
MASSACHUSETTS INSTITUTE OF TECHNOLOGY
CAMBRIDGE, MASSACHUSETTS

The research reported in this document was made possible through support extended the Massachusetts Institute of Technology, Research Laboratory of Electronics, jointly by the Army Signal Corps, the Navy Department (Office of Naval Research) and the Air Force (Air Materiel Command), under Signal Corps Contract No. W36-039-sc-32037, Project No. 102B; Department of the Army Project No. 3-99-10-022.

MASSACHUSETTS INSTITUTE OF TECHNOLOGY

RESEARCH LABORATORY OF ELECTRONICS

Technical Report No. 175

September 11, 1950

LOCKING PHENOMENA IN MICROWAVE OSCILLATORS WITH MISMATCHED LOADS

Joseph C. Pitts
William F. Wicks
Edward E. David, Jr.

Abstract

This report is a supplement to Technical Report No. 63. It presents an exact graphical method for predicting the behavior of an oscillator, perturbed by an external signal and operating into an arbitrary but passive load impedance. The method is applicable to any oscillator, but is applied here to a reflex klystron. Both theoretical and experimental results are included.

LOCKING PHENOMENA IN MICROWAVE OSCILLATORS WITH MISMATCHED LOADS

I. Introduction

This paper is intended as a supplement and continuation of Technical Report No. 63 (ref. 3). In particular, sec. 6 of that report has been found to be in error and this material should supersede that section. Briefly, Technical Report No. 63 shows how the behavior of an oscillator, perturbed by an external signal, may be predicted. The analysis there is based on the assumption that the passive load of the oscillator is matched to its transmission line. This report shows how to extend that analysis to include passive mismatched and resonant loads.

II. Summary of Matched Load Analysis

Technical Report No. 63 shows how the Rieke diagram of an oscillator uniquely specifies the oscillator operation as a function of the load admittance, provided the d-c conditions are fixed. Any point on the diagram corresponds to a load admittance, a power output, and a frequency of oscillation.

If a microwave oscillator is operating into a matched load, its operating conditions are specified by the output power and frequency contours passing through the center of the Rieke diagram where the reflection coefficient is zero. If, then, a locking signal of frequency, ω_1, and of sufficient amplitude, is injected into the output line, the oscillator will change its frequency from the initial frequency ω' to the locking signal frequency of ω_1, provided ω_1 is not too different from ω'. This change in frequency is accompanied by a change in output power and r-f operating conditions, but the d-c conditions remain unchanged since they are controlled externally.

The operating frequency will track the locking signal frequency until the difference $|\omega_1 - \omega'|$ becomes too large, at which time the oscillator breaks synchronism.

When the oscillator shifts frequency from ω' to the frequency ω_1 of the locking signal, the point of operating on the Rieke diagram shifts to the new frequency contour where the reflection coefficient has a value greater than zero, and is given by

$$\rho = |\rho| e^{j\theta} = \frac{E_s}{E_i} = \sqrt{\frac{P_s}{P_i}} e^{j\theta} \qquad (1)$$

where

E_s = value of synchronizing voltage
P_s = magnitude of synchronizing power
E_i = value of oscillator incident voltage
P_i = magnitude of oscillator incident power

This change of reflection coefficient reveals the mechanism of oscillator synchronization; when locking to an external signal, the oscillator assumes a phase and power output for which the resulting coefficient, as given by Eq. 1, specifies the frequency ω_1. As ω_1 is changed, therefore, the reflection coefficient varies in a manner

determined by the load characteristics of the oscillator.

Since the characteristics of the electronic discharge are inherent in the Rieke diagram, they do not affect the mechanics of the locking action. As a result, an analysis of this type is applicable to any oscillator.

Consider the reflection coefficient plane, with contours of constant power output superimposed upon it. Each point in the plane corresponds to a unique reflection coefficient ($|\rho| e^{j\theta}$) and power output. It may be shown that

$$P_o = P_i - P_s$$

and

$$P_s = |\rho|^2 P_i$$

therefore

$$P_s = \frac{P_o |\rho|^2}{1 - |\rho|^2}$$

where

P_o = power output

P_i = power in incident wave

P_s = power in reflected wave

$|\rho|$ = magnitude of reflection coefficient

Thus each point in the plane also represents a unique reflected power. Contours of constant reflected power then may be constructed from the Rieke diagram on the reflection coefficient plane. These contours represent the variation of load admittance required to maintain constant reflected power as the incident wave changes magnitude and phase with frequency. Lines of CRP (constant reflected power), therefore, represent the path of klystron locked operation as a function of frequency, with locking power as a parameter.

III. Mismatched Load Analysis

Mismatched loads are almost unavoidable in a practical system. To illustrate the effects of a mismatched load on the preceding analysis, consider the circuit shown below, operating under the following conditions:

1. The synchronizing signal propagates only toward O_L.
2. There is no wave propagating toward O_S.
3. The amplitude, phase, and frequency of the injected signal may be varied independently and all are independent of the operation of O_L.

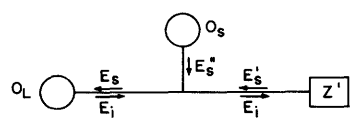

where

O_S = source of locking signal

O_L = oscillator to be locked

Z' = normalized equivalent impedance lumping the load and insertion impedance of O_S.

E''_s = synchronizing wave supplied by O_S.

For this system the equivalent reflected signal incident on O_L will be made up of two components, one due to the synchronizing wave E''_s and the other due to the reflected wave, E'_s, from the mismatched load. Vectorially then

$$\vec{E}_s = \vec{E}'_s + \vec{E}''_s$$

and the reflection coefficient ρ presented to the locked tube is

$$\vec{\rho} = \frac{\vec{E}_s}{\vec{E}_i} = \frac{\vec{E}'_s + \vec{E}''_s}{\vec{E}_i} = \vec{\rho}' + \vec{\rho}'' \quad .$$

or

$$|\rho| e^{j\theta} = |\rho'| e^{j\theta'} + |\rho''| e^{j\theta''}$$

but

$$\sqrt{|\rho''|} = \left|\frac{E''_s}{E_i}\right| = \sqrt{\frac{P''_s}{P_i}}$$

thus

$$\sqrt{\frac{P''_s}{P_i}} e^{j\theta''} = |\rho| e^{j\theta} - |\rho'| e^{j\theta'} \quad . \tag{2}$$

Let

$$|\rho_R| e^{j\theta_R} = \rho e^{j\theta} - |\rho'| e^{j\theta'}$$

$$\sqrt{\frac{P''_s}{P_i}} e^{j\theta''} = |\rho_R| e^{j\theta_R} \tag{3}$$

Therefore

$$\theta'' = \theta_R \tag{4}$$

and

$$\sqrt{\frac{P''_s}{P_i}} = \rho_R \quad . \tag{5}$$

On the Rieke diagram are located contours of constant output power P_o, but

$$P_o = P_i - P_s$$

and, as before

$$P_s = |\rho|^2 P_i$$

or

$$P_i = \frac{P_o}{1 - |\rho|^2} . \tag{6}$$

Combining Eqs. 5 and 6

$$P_s'' = \frac{P_o |\rho_R|^2}{1 - |\rho|^2} . \tag{7}$$

The CRP contours derived in the previous section are contours of constant P_s, whereas with a mismatched load P_s'' is constant, while P_s is dependent on the load and injected power. Therefore, the CRP contours are no longer the operating locus for constant amplitude locking signals. However, the plot of Eq. 7 on the Rieke diagram for constant P_s'' and a particular load is the locus of operating points of the oscillator. It is seen from Eqs. 2, 3 and 7 that P_s and P_s'' become identical when there is no mismatch ($\rho' = 0$).

Since the CRP contours are fundamentally a characteristic of the oscillator itself, just as the Rieke diagram is determined by the electronics of the oscillator, the locking characteristics, expressed by the CRP contours, are inherently specified by the tube design. On the other hand, the loci expressed by Eq. 7 are a function of the load impedance Z'; hence they are dynamic loci characterized by the system external to the oscillator. Consequently, they will be referred to as dynamic-load contours, or simply as DL contours.

IV. Application to a Nonfrequency-Sensitive Mismatched Load

As was seen in the preceding section, a particular DL contour is applicable only for a specific load. The mismatch used in the experimental investigation was that introduced by a directional coupler. Once the reflection coefficient ($|\rho'| e^{j\theta'}$) of this mismatch was determined, the DL contours can be calculated from the Rieke diagram (see Sample Calculations for detailed procedure). The value of $|\rho'| e^{j\theta'}$ was measured (as will be described in the next section). It was found to be $0.11\, e^{j43.2^\circ}$ and was essentially constant over the range of frequencies of the Rieke diagram.

The calculated DL contours for this mismatch are shown in Fig. 2, having been calculated from the Rieke diagram of Fig. 1. Also shown in Fig. 2 are CRP contours for the same values of synchronizing power. The comparison shows that there is considerable difference in the location of these sets of contours, each of the DL contours

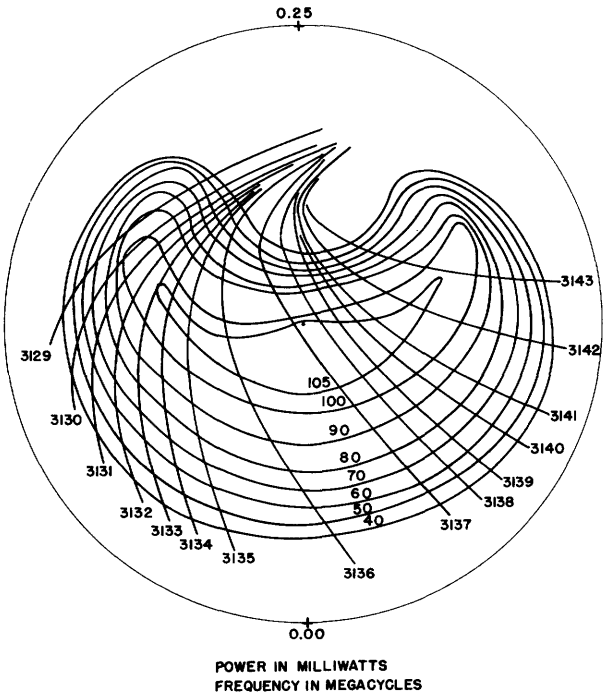

Fig. 1

Rieke diagram of 707-B klystron
repeller voltage = −150 volts
anode voltage = 217 volts

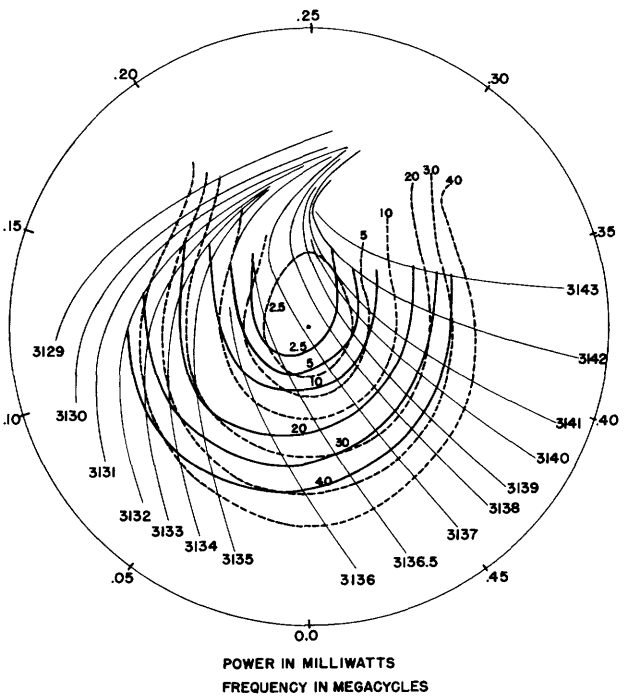

Fig. 2

Constant reflected power and dynamic load contours
---constant reflected power (matched load)
——dynamic load contour with reflection coefficient = 0.11, phase angle = 0.19λ

having been displaced in an upper left-hand direction. Notable is the fact that the displacement was in the direction of the reflection coefficient vector of the load $|\rho'| e^{j\theta'}$.

From this, it can be concluded that if the mismatch is of the right magnitude and phase, any DL contour can be made to pass through the origin. Hence, an oscillator may be synchronized and also operate into a matched load, if the locking frequency and the passive load impedance are correctly chosen.

V. Experimental Verification

Having calculated the operating paths of the oscillator on the Rieke diagram, it is desirable to verify these paths experimentally.

The circuit used for the experimental investigation of the DL contours is shown in Fig. 3. The synchronizing signal source was a QK-61 tunable magnetron. Its output was directed into a matched power divider which shunted most of the power into a matched power divider which shunted most of the power into a matched load, where it was dissipated. A small portion of the power passed through a directional coupler where its value was measured by a thermistor bridge. From there it was attenuated 13.1 db as it passed through a second directional coupler, from which it emerged as the locking signal which was incident on the output line of the tube to be locked (707B klystron, in this case).

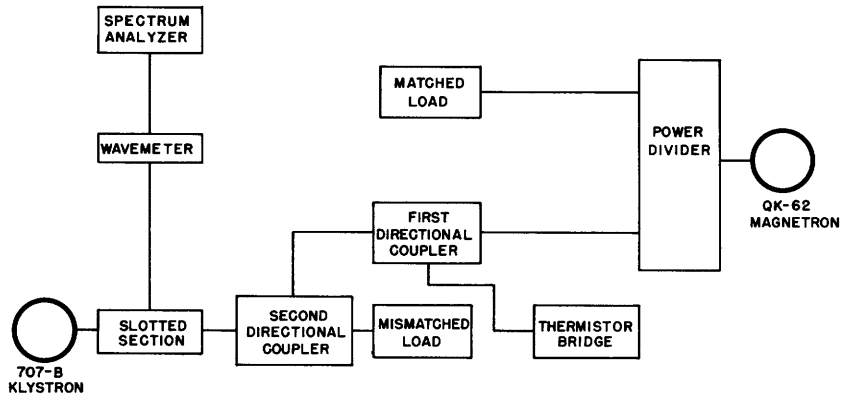

Fig. 3
Experimental circuit

Since the maximum synchronizing signal at the locked tube was 40 mw (maximum value used for calculated curves), and the total magnetron output was about 60 watts, the attenuation between the two tubes was never less than 32 db. Therefore, the operation of the magnetron was independent of the 707B system. There were essentially no reflections from the second directional coupler, hence the incident power was proportional to the synchronizing signal.

To determine the reflection coefficient presented to the 707B, standing wave measurements were made in a slotted section between the tube and the mismatched second directional coupler. The magnitude of the SWR was measured by means of a probe-coupled spectrum analyser, and the phase was determined by a vernier on the probe carriage. Frequency was measured with a coaxial wavemeter, connected in series between the probe of the slotted section and the spectrum analyzer.

To obtain points on the DL locking contours, the repeller and accelerator voltages on the klystron had to be set and maintained at the same values for which the Rieke diagram applies. As the frequency of the magnetron was varied, the injected power was adjusted for a particular value, and measurements were made of SWR, minimum position and frequency. From this information it was possible to plot the experimental points on the Rieke diagram.

Before the DL contours could be calculated, it was necessary to measure the amount of mismatch which was presented to the klystron with no locking signal applied. This was done by arranging the equipment as described, but using a signal generator in place of the 707B to investigate possible frequency sensitivity of the load. The magnetron power was off except for the filament supply. It was found that the reflection coefficient of the mismatch was constant in amplitude (= 0.11) and its phase changed very slightly (approximately 0.02λ on the Smith chart) over the range of frequencies of the Rieke diagram. Had the length of the transmission line been longer, the variation of phase would have been greater and corrections would have been necessary. The reflection coefficient of the mismatched load was found also to be independent of the setting of power divider

and of the tuning of the magnetron cavity. Consequently, it was assumed that the passive load was constant and independent of all variables.

The comparison between experimental points and the calculated contours is shown in Fig. 4, where the experimental points are superimposed on the calculated DL contours. The close agreement between the two shows the analysis to be correct. The small discrepancies are attributed to experimental errors of which the most important is the temperature-humidity variation factor. Especially sensitive in this respect are the power measurements with the thermistor bridge. Also, temperature changes affect the klystron characteristics as well as the wavemeter readings. The largest deviations of the experimental results are at small values of injected power. This is due in part to errors in the calculations because of the nature of the Rieke diagram in that region.

The experimental locking boundaries are also shown in Fig. 4. Theoretically, the locking boundaries are the points of tangency between frequency contours and the DL or CRP contours. Due to the absence of frequency contours in these regions, except for small values of synchronizing power, it was not possible to compare the experimental and theoretical locking boundaries of the DL contours or to make any comparison with the theoretical boundaries for the CRP contours.

VI. Application to Resonant Loads

This graphical analysis may be applied to frequency-sensitive mismatched loads. As an example, consider an oscillator operating into a resonant cavity, the constants of which have been determined by cold test (2). For this system, the calculation of the DL contours is only slightly more complicated than for a nonfrequency sensitive mismatched load.

The approximate input impedance of a resonant cavity is (2)

$$Z = \frac{1/Q_{ext}}{j\left(\frac{\omega}{\omega_o} - \frac{\omega_o}{\omega}\right) + 1/Q_o} + Z_1 \tag{8}$$

where Z is the ratio of the impedance to the characteristic impedance of the guide. The quantity Q_o is the unloaded Q of the cavity, while Q_{ext} is a measure of the coupling of the cavity to the output. Z_1 is a very small real quantity which can be neglected, although for 1-cm and 3-cm magnetrons it is not entirely negligible. The resonance frequency is ω_o. By replacing the term $(\omega/\omega_o) - (\omega_o/\omega)$ by $2(\omega - \omega_o/\omega_o)$, which is an excellent approximation near resonance, one may rewrite Eq. 8 as

$$Y = \frac{1}{Z} = \frac{Q_{ext}}{Q_o} + j2Q_{ext}\frac{(\omega - \omega_o)}{\omega_o} \tag{9}$$

For each frequency on the Rieke diagram of the tube whose locking characteristics is to be determined, Eq. 9 gives a particular G + jB for the input admittance of the

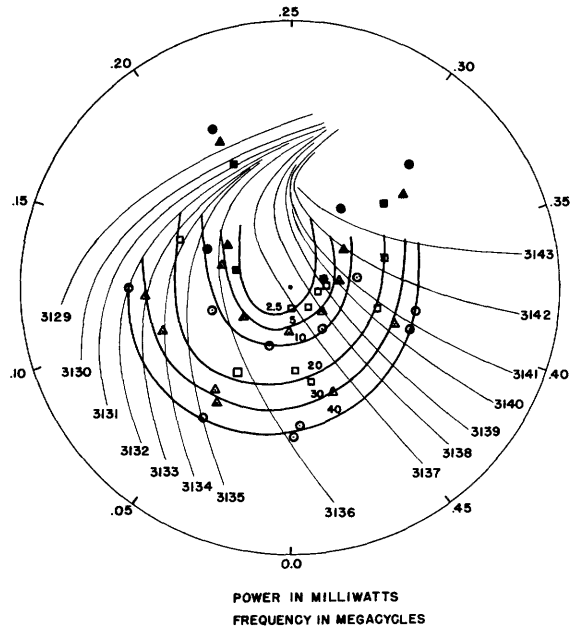

Fig. 4

Theoretical dynamic load contour for load with reflection coefficient = 0.11, and phase angle = 0.19λ
Experimental points are shown

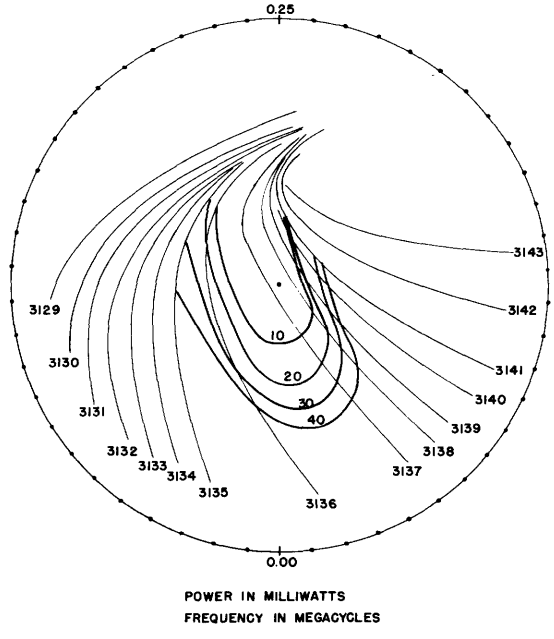

Fig. 5

Theoretical DL contours for resonant load
Q_{ext} = 563 Q_o = 450
Q_{eff} = 250 f_o = 3137 Mc
Line length = 0

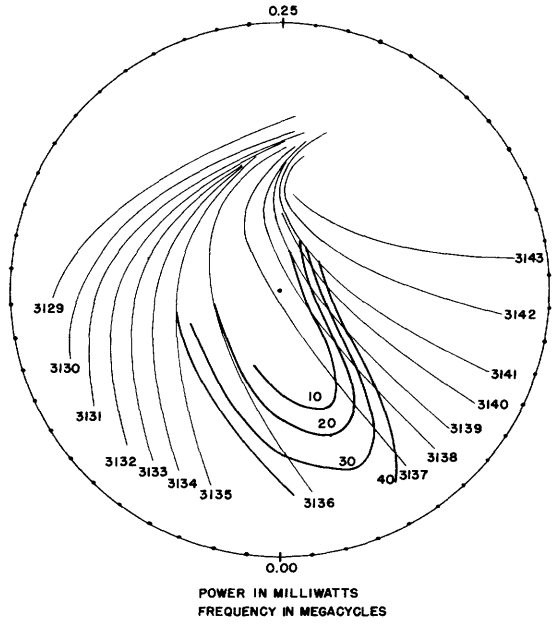

Fig. 6

Theoretical DL contours for resonant load
Q_{ext} = 450 Q_o = 563
Q_{eff} = 250 f_o = 3137 Mc
Line length = 0

resonant cavity load. The G, obviously, will be determined by the ratio of Q_{ext}/Q_o and is either equal to or the inverse of the standing wave magnitude, depending upon how the cavity is loaded. Since the Rieke diagram was drawn on an admittance plane, admittances rather than impedances must necessarily be used in the calculations. The apparent load admittance on the tube is dependent upon the length of line to the cavity load, as with any transmission line.

With the apparent load admittance at each frequency and the Rieke diagram, it is now possible to calculate the DL contours (see Sample Calculations for further details).

To illustrate the effect of resonant cavity loads on the CRP contours, DL contours were calculated for cavities having various combinations of Q_{ext} and Q_o. These effects were found to vary greatly for the combinations chosen, but observations can be made from which the general shape and approximate location of the DL contours can be predicted for any load.

Figure 5 is drawn for an undercoupled cavity load having $Q_{ext} = 563$ and $Q_o = 450$. The effective (loaded) Q, which is given by $1/Q_{ext} + 1/Q_o$, is 250 and was chosen approximately equal to the klystron's loaded Q of about 210. The conductance of the load ($= Q_{ext}/Q_o$ from Eq. 9) is 1.25. Since the line length was assumed to be zero, the locus of the load admittance of the klystron is the G = 1.25 circle on a Smith chart used as an admittance plot. When the points, corresponding to the admittances at each frequency of the Rieke diagram, are plotted on this locus with $f_o = 3137$ mcps (the frequency line passing nearest the center of the Rieke diagram), it can be seen that vectors from the origin to these points are fan shaped upward. These vectors are the load reflection coefficient vectors at the corresponding frequencies. The magnitude of these reflection coefficient vectors varied from 0.11 at f_o to 0.63 at the frequencies $\pm$ 5 Mc from f_o. Observing Fig. 5 it is seen that the DL contours are displaced slightly upward around the center frequency from the location of the CRP contours. Note that this is in the same direction as the load reflection coefficient vector at the resonant frequency. Further, the sides are pulled in toward the center in accordance with the same rule, since the reflection coefficient vectors point in an upper right direction for frequencies in the lower lefthand corner of the Rieke diagram, and vice versa. Contours of higher P_s'' could have been drawn in the areas outside the contours.

The DL contours of Fig. 6 are drawn for the same loaded Q of 250 but with the Q_{ext} and Q_o values reversed, the overcoupled case. This reversal had the effect of pulling down at the resonant frequency and rounding the bottom slightly. This is in exact accordance with the previous explanation that the part of the CRP contour near any frequency contour is pulled in the direction of the load reflection coefficient vector of that same frequency. The load reflection coefficient vectors are drawn for this case in Fig. 7. Here it is seen that the vectors, down near f_o, increase in length and fan out upward on both sides of f_o.

Figure 8 is drawn for a greatly undercoupled cavity having Q_{ext} of 500, Q_o of 250, Q_{eff} of 167, and a quarter-wave length line. This case is interesting in that it shows

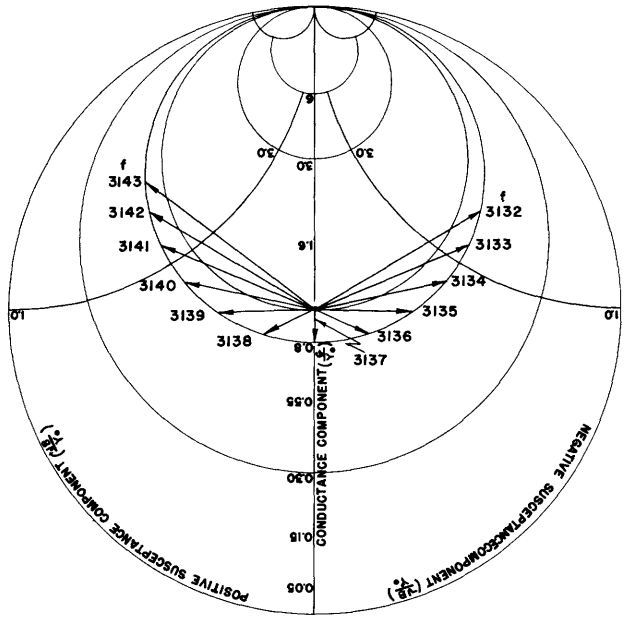

Fig. 7

Load reflection coefficient as a function of frequency

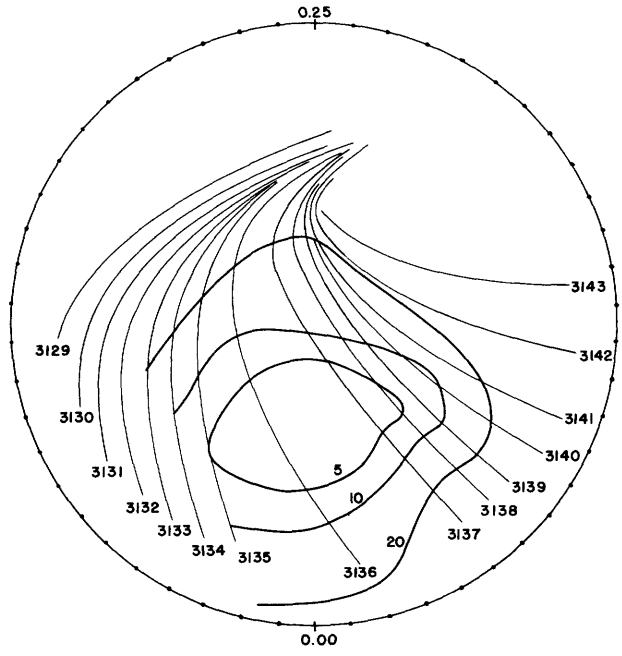

POWER IN MILLIWATTS
FREQUENCY IN MEGACYCLES

Fig. 8

Theoretical DL contour for resonant load

Q_{ext} = 500 Q_o = 250

Q_{eff} = 167 f_o = 3137 Mc

Line length = $\lambda/4$

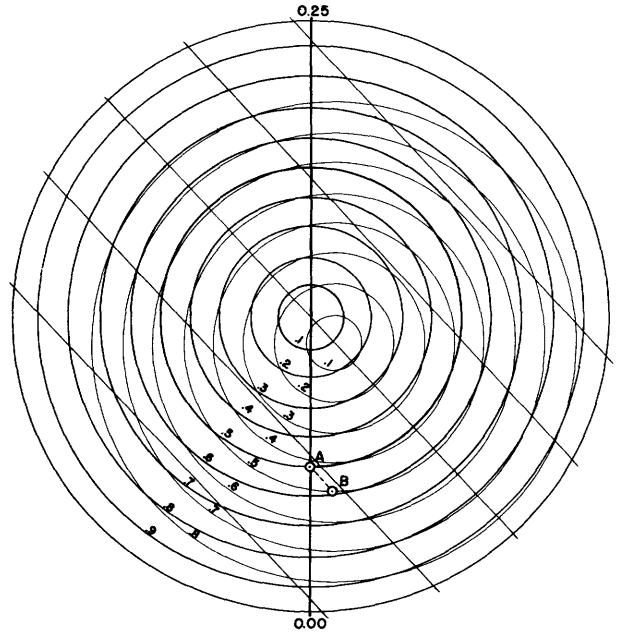

GRAPHICAL SOLVER

Fig. 9

Graphical solver

two operating points. The fact in itself is not so startling since in DL contours for other cases, two operating points have been seen, but in the other case the contour has encircled the origin.

In Technical Report No. 63, it has been stated and verified experimentally that for a CRP contour that encircles the origin, the stable operating point will be that point on a contour crossing the frequency line where $df/d\theta$ is positive. This statement was proved in the following manner

$$\theta = \psi - \phi \tag{10}$$

where

ψ = phase of synchronizing signal

ϕ = phase of generated wave.

Differentiating

$$\frac{d\theta}{dt} = \frac{d\phi}{dt} = -\Delta\omega \tag{11}$$

since ψ is constant. A random positive dynamic rate of change in ϕ results in a positive change, $\Delta\omega$, and a negative change, $-d\theta/dt$. Operating points in the "sink region" of the Rieke diagram move in a cumulative manner under these conditions and are therefore unstable. On the other hand, on the lower operating path the negative $d\theta/dt$ produces a negative $\Delta\omega$, which conflicts with Eq. 11, making those operating points stable. The locking boundaries are then the points on a CRP contour where the CRP and frequency contours are tangent, since at these points $df/d\theta = 0$.

It seems that this same criterion can be applied to the case of Fig. 8, where the entire path is below the center of the Rieke diagram. Here, both the upper and lower paths are stable according to this criterion. If the locking region is approached from either side by frequency change, at the point of tangency it would seem that the oscillator would be free to assume either operating point. If the locking region is approached by decreasing the amount of injected power and following a freqency line in, the approach would be inevitably from the bottom toward the lower paths. This is due to the fact that the larger power contours encircle the origin and only their lower paths are stable operating points. Should the contour be approached by increasing the injected power from zero, it would be possible to operate on either path.

Since, in this case, the line length was assumed to be a quarterwave length, the admittance locus (G = 2 circle) was rotated a quarterwave length on the Smith chart. This then made the reflection coefficient vectors all fan downward. The relatively large reflection coefficients (the minimum is 0.33) cause the pulling of the DL contours to be so great that the largest complete contour that could be plotted was the 20 Mw contour. Also notable is the fact that the contours seem to have been compressed from the top and bottom. This fact is again in line with previous tendencies, since now the load reflection coefficient vectors and corresponding frequency lines lie in the same quadrants. As can be seen, the CRP contours have been pulled down in the center,

down and slightly to the right on the right side, and correspondingly on the left side.

It is possible that for particular loads, some of the DL contours will be entirely in the unstable regions of the Rieke diagram. For values of synchronizing power tending to put the operating point on such a contour, synchronization would not take place at all, although some interaction would be evident. Probably this interaction would take the form of a frequency modulation of the oscillator.

In conclusion, it has been seen that the behavior of a synchronized oscillator may be predicted, whatever its passive load impedance.

Sample Calculations

A. Theoretical DL contours for nonfrequency sensitive load

A table was made for each frequency line on the Rieke diagram noting the phase and θ, and the output power for each even value of $|\rho|$. Even values were chosen for simplicity.

Since, in the calculations, it was necessary to subtract a vector of constant amplitude and phase (reflection coefficient of load) from a vector of varying length and phase (various $|\rho| e^{j\theta}$'s on the Rieke diagram), a graphical solver, shown in Fig. 9 was made to expedite the calculations. Figure 9 is made up of circles concentric about the origin, corresponding to constant reflection coefficient circles on a Smith chart, upon which is superimposed another set of circles concentric about a point which is offset from the center by an amount equal to $|\rho'|$ (= 0.11), at an angle of θ' (= 0.44) which is the negative of the vector represented by $|\rho'| e^{j\theta}$. Then for each value of $|\rho| e^{j\theta}$, $|\rho_R|$ was obtained by moving from the point $|\rho| e^{j\theta}$, on the circles concentric about the origin, parallel to the line joining the centers, in the direction of the offset center to the corresponding point on the offset circle of the same radius and reading $|\rho_R|$ on the circles concentric about the origin. For example, if $|\rho| e^{j\theta} = 0.5 e^{j\theta}$ (Point A on Fig. 10), then $|\rho_R| = 0.59$ (Point B).

Then for each value of $|\rho| e^{j\theta}$, P_o and $|\rho_R|$ were known, and P_s'' was calculated from Eq. 7. For each frequency, P_s'' then was plotted as a function of $|\rho|$. The minimum $|\rho|$ for each frequency, which could be determined from the Rieke diagram, was very helpful in drawing these curves. The DL contours were then drawn for various values of P_s'' through the points at which each frequency line was intersected by the circle of radius $|\rho|$ corresponding to the particular P_s''.

Following is the table made for the f = 3135 Mc contour of the Rieke diagram

$\|\rho\|$	θ	P_o (Mw)	$\|\rho_R\|$	P_s'' (Mw)
0.7	0.033	47	0.75	52
0.6	0.045	64	0.64	41
0.5	0.063	83	0.52	30
0.4	0.098	102	0.37	16.6
0.4	0.184	72	0.29	7.2
tan 0.37				

$|\rho|$ is the radius of the constant reflection coefficient circles drawn on the Rieke diagram, θ is the phase angle corresponding to the intersection of the reflection coefficient circles and the f = 3135 Mc line, P_o is the output power at this intersection, $|\rho_R|$ is the magnitude of the resultant vector which is obtained from the graphical solver of Fig. 9, and P_s is obtained from Eq. 7 which is

$$P_s'' = \frac{|\rho_R|^2}{1 - |\rho|^2} P_o$$

B. Theoretical DL contours for resonant cavity loads

The calculation of these contours is very similar to that for the nonfrequency-sensitive load. In this case the load admittance as seen by the tube at each frequency is different, thus making the $|\rho'| e^{j\theta'}$ different. Tables were made for each frequency, as in the previous case. To find $|\rho_R|$, a graphical solver had to be constructed so that the position of the center of the offset circles was movable. This was necessary because now both vectors to be added are of variable lengths and phases. This new solver was made by drawing one set of concentric circles on thin paper, permitting the other set, drawn on another sheet of paper and placed underneath, to be shifted by any amount relative to the top set of circles. The position of the center of the offset circles was then changed for each frequency, and the solutions were found in exactly the same way as in Fig. 9.

For any frequency, the position of the center of the offset circles was at the terminus of the negative of the load reflection coefficient vector for that frequency expressed as a magnitude at a phase angle as read on the Smith chart.

References

1. W. H. Bostick, E. Everhart, M. Labitt: Parallel Operation of Magnetrons, Technical Report No. 14, Research Laboratory of Electronics, M.I.T., Sept., 1946
2. J. C. Slater: The Phasing of Magnetrons, Technical Report No. 35, Research Laboratory of Electronics, M.I.T., April, 1947
3. E. E. David, Jr.: Locking Phenomena in Microwave Oscillators, Technical Report No. 63, Research Laboratory of Electronics, M.I.T., April, 1948